Junctophilin-2 expression rescues atrial dysfunction through poly-adic junctional-membrane-complex biogenesis

Research Manuscript

Sören Brandenburg[1], Jan Pawlowitz[1], Benjamin Eikenbusch[1], Jonas Peper[1], Tobias Kohl[1], Gyuzel Y. Mitronova[2], Samuel Sossalla[1§], Gerd Hasenfuss[1,3], Xander H.T. Wehrens[4], Peter Kohl[5], Eva A. Rog-Zielinska[5], Stephan E. Lehnart[1,3,6]✉

[1] Heart Research Center Göttingen, Department of Cardiology & Pneumology, University Medical Center Göttingen, Göttingen, Germany; [2] Department of NanoBiophotonics, Max Planck Institute for Biophysical Chemistry, Göttingen, Germany; [3] DZHK (German Centre for Cardiovascular Research), partner site Göttingen, Germany; [4] Cardiovascular Research Institute – Department of Molecular Physiology and Biophysics, Baylor College of Medicine, Houston, TX, United States; [5] University Heart Center, Faculty of Medicine, University of Freiburg, Freiburg im Breisgau, Germany; [6] BioMET, Center for Biomedical Engineering and Technology, University of Maryland School of Medicine, Baltimore, Maryland, USA.

*** Correspondence:**
Stephan E. Lehnart
slehnart@med.uni-goettingen.de

[§] New address: Department for Internal Medicine II, Cardiology, Pneumology, Intensive Care, University Hospital Regensburg, Regensburg, Germany.

Supplemental Material

1. Supplemental Methods

2. Supplemental Figures and Figure Legends

3. Supplemental Tables

Supplemental Methods

Mouse models, genotyping, and tamoxifen treatment

Animal procedures were reviewed by the institutional animal care and use committee and approved by the veterinarian state authority (LAVES) in compliance with the human care and use of laboratory animals. Unless indicated otherwise, we used adult gender-mixed mouse cohorts of 10-16 weeks age back-crossed into the C57BL/6N background. The generation of both the junctophilin-2 knock-down (MCM-shJP2) and junctophilin-2 overexpression (JP2-OE) mouse strains was previously described (1). For genotyping by PCR we used the following primer pairs: MCM, 5'-AGGTGGACCTGATCATGGAG-3' and 5'-ATACCGGAGATCATGCAAGC-3', resulting in a 440 bp fragment; shJP2, 5'-CGAAGTTATCTAGAGTCGAC-3' and 5'-GCTATGACCATGATTACGCCA-3', resulting in a 250 bp fragment; and JP2-OE, 5'-AGAAGGGCCGTAAGGAAGTG-3' and 5'-TAGAAGGCACAGTCGAGG-3', resulting in a 200 bp fragment. For junctophilin-2 knock-down, single-transgenic αMHC-MerCreMer (MCM) mice and double-transgenic MCM-shJP2 mice were treated once by intraperitoneal injection of 40 mg tamoxifen/kg body weight. For this, 10 mg tamoxifen (T5648, Sigma Aldrich) were dissolved in 100 µl ethanol, and diluted 1:10 in soybean oil (S7381, Sigma Aldrich). For details about the protocol selection for atrial junctophilin-2 knock-down please see Supplemental Figure 3.

Human myocardial samples

Human tissue samples for immunofluorescence imaging were obtained from the right atrial appendage, left atrium or the left ventricle of patients undergoing open heart surgery for coronary bypass grafting or aortic valve replacement. Please see Supplemental Table 3 for details about the clinical patient information. Left atrial and left ventricular tissue samples for Western blot analysis were obtained from explanted human hearts. All patients provided

written informed consent and the protocol was reviewed and approved by the Ethics committee of the University Medical Center Göttingen (No. 21/10/00).

Transaortic constriction in mice

Minimally invasive transaortic constriction (TAC) was performed in 8-12 week old mice (2, 3). Mice were anesthetized with 1.5–2 % isoflurane in oxygen using a rodent ventilator. For permanent constriction, a 27 G spacer and a 5-0 polyviolene suture were used. Sham operated animals underwent the same procedure, but without constricting the suture. Body temperature, respiration rate, and surface ECG were monitored throughout the procedure. The hemodynamic gradient was measured 2 days post-TAC. Please see below for details about the echocardiographic procedures. Fentanyl and carprofen were injected subcutaneously prior to surgery; in addition, buprenorphin (0.1 mg/kg body weight) twice, prior and 8 hours after surgery; and carprofen (5 mg/kg body weight) 24 hours after surgery. Mice that died within 48 hours post-TAC from perioperative complications were excluded from further survival analysis. Finally, to induce junctophilin-2 knock-down post-TAC, tamoxifen was injected on the third post-operative day as described above and in Supplemental Figure 3.

Cardiac myocyte isolation from mouse hearts

Mice were anesthetized with isoflurane followed by cervical dislocation and heart extraction. For isolation of atrial and ventricular myocytes from mouse hearts we used a modified Langendorff perfusion setup. First, a nominally Ca^{2+} free perfusion buffer (Supplemental Table 2) was perfused, followed by a collagenase type II (Worthington) in perfusion buffer as described previously (3, 4). To document sufficient quality of isolated cells and to analyze atrial myocyte dimensions (cell length, width, length-to-width ratio, and cell area), we used transmitted light imaging (Zeiss LSM 710 and 880, Jena, Germany) and Fiji (https://imagej.net/Fiji) (4).

Confocal and STED immunofluorescence microscopy

Isolated cardiomyocytes plated on laminin-coated coverslips were fixed with 4% PFA for 5 minutes followed by three PBS washing steps. Next, fixed samples were incubated overnight in blocking/permeabilization buffer (10% v/v bovine calf serum and 0.2% v/v Triton X-100 in PBS). Primary antibodies were diluted in blocking buffer and incubated on cell samples overnight at 4 °C. For detailed primary antibody information please refer to Supplemental Table 1. After washing three times in blocking buffer, samples were incubated with secondary antibodies diluted 1:1000 for 2 h at room temperature.

Different secondary antibody protocols were used. For confocal co-immunofluorescence microscopy a goat anti-rabbit Alexa Fluor 633 and a goat anti-mouse Alexa Fluor 514 (A-31555, A-21071, Thermo Fisher Scientific); for triple staining in Supplemental Figure 2 a goat anti-rabbit Alexa Fluor 514, a goat anti-mouse Alexa Fluor 568, and a Zenon Alexa Fluor 647 rabbit IgG labeling kit (Z25308, Thermo Fisher Scientific) were used according to the original manufacturer's instruction. For STED microscopy, a goat anti-rabbit STAR 635P (2-0012-007-2, Abberior), a goat anti-mouse STAR 580 (2-0002-005-1, Abberior), or a goat anti-mouse STAR 488 (2-0002-006-8, Abberior) antibody were used; for triple staining in Supplemental Figure 10, samples were incubated with donkey anti-goat STAR 580 (Abberior) and washed thrice in blocking buffer prior to incubation with goat anti-rabbit STAR 635P (2-0012-007-2, Abberior) and goat anti-mouse STAR 488 (2-0002-006-8, Abberior).

Next, a second PBS wash-step was repeated three times and cardiac myocytes were embedded in DAPI-free mounting medium (ProLong Gold Antifade Mountant, Thermo Fisher Scientific). Confocal images were acquired with a Zeiss LSM 710 microscope and a Plan-Apochromat 63x/1.40 oil objective using a pixel size of 100 x 100 nm. For STED imaging we used a Leica TCS SP8 system and a HC PL APO C2S 100x/1.40 oil objective. The STED

workflow was optimized for the STAR 635P and STAR 580 fluorophores using the following parameters: pixel size 16.23 x 16.23 nm, pixel dwell time 400 ns, scanning speed 600 Hz, 32x line averaging, excitation by a white-light laser at 635 and 580 nm, STED depletion at 775 nm, and fluorescence detection between 650-700 nm and 600-630 nm. For STAR 488 antibody labeling we used STED depletion at 592 nm, and fluorescence detection between 515-560 nm. The STED laser power was adjusted to maximize resolution. Raw images were processed in Fiji (https://imagej.net/Fiji). Image contrast of confocal and STED images was adjusted using the identical setting for group comparison. For STED image analysis please refer to the next chapter.

3D cluster reconstruction/projection for Figures 1C and 1D was computed using the Fiji 3D Viewer after signal binarization. Yellow-colored signals represent the merged signal between the RyR2 (red) signal overlapping either with the junctophilin-2 or RyR2-pS2808 (green) signal, respectively. The unspecific (cross-reaction) nuclear RyR2-pS2808 antibody signal described previously (3) was used to visualize the nucleus (blue) in Figure 1D.

JP2 and RyR2 cluster analysis of STED images

Quantitative analyses of subcellular JP2 and RyR2 cluster properties were based on STED immunofluorescence imaging as described above. The immunofluorescence signal pattern of junctophilin-2 or RyR2 was segmented by two distinct Fiji operations (https://imagej.net/Fiji): 1) junctophilin-2 images (STAR 635P) were background subtracted (rolling ball radius: 35 pixels), smoothed (Gaussian, sigma 1 pixel), and global Otsu thresholding was used to binarize the junctophilin-2 signals. 2) RyR2 images (STAR 580 used to compare Sham vs. TAC and WT vs. JP2-OE; STAR 488 for AM vs. VM and MCM vs. MCMshJP2) were background subtracted (rolling ball radius: 25 pixels for STAR 488; 35 pixels for STAR 580), local contrast enhanced, and smoothed (Gaussian, sigma 1 pixel). Processed images were

segmented by local Bernsen thresholding (15 pixel radius). For both junctophilin-2 and RyR2 signals, binarized images were used to determine the signal area fraction, cluster density, and cluster area. For overlap analysis between junctophilin-2 and RyR2 clusters, we accepted clusters that ranged between partial up to mutually complete overlap in binarized images. Statistical analysis was based on the number of mouse hearts.

$Ca_V1.2$ cluster analysis of STED images

For quantitative assessment of the $Ca_V1.2$ cluster area on axial tubules, AMs from WT and JP2-OE hearts were immunostained with $Ca_V1.2$ and caveolin-3 antibodies and imaged with STED microscopy as described above. The immunofluorescence signal patterns of $Ca_V1.2$ and caveolin-3 were segmented in ImageJ/Fiji (https://imagej.net/Fiji): $Ca_V1.2$ (STAR 635P) and caveolin-3 images (STAR 580) were background subtracted (rolling ball radius: 15 pixels), smoothed (Gaussian, sigma 1 pixel), and processed images were segmented by global Otsu thresholding. Then, binarized images were used to determine the cluster area of $Ca_V1.2$ signals overlapping with caveolin-3 signals as a tubular marker protein. For overlap analysis between $Ca_V1.2$ and caveolin-3 clusters, we accepted clusters that ranged between partial up to mutually complete overlap in binarized images. Statistical analysis was based on the number of mouse hearts.

STED microscopy of human myocardial tissue sections

For STED imaging, human cardiac tissue samples obtained as described above underwent fixation overnight (Roti-Histofix 4 %, Carl Roth, Germany), were embedded in paraffin, and cut into 4 µm thick histological sections. Following deparaffinization and rehydration, antigens were unmasked in 10 mM sodium-citrate buffer prior to antibody incubation. Next, samples were blocked and permeabilized by PBS containing 4% BSA and 0.1% Triton-X100 for 1 hour. Primary antibodies were diluted in PBS containing 4% BSA and samples

incubated overnight in a custom-made wet chamber at room temperature as follows: rabbit anti- junctophilin-2 1:250 (40-5300, Thermo Fisher Scientific), and mouse anti-caveolin-3 1:250 (610421, BD Biosciences). Following washing, samples were incubated with secondary antibodies for 2 hours at room temperature: goat anti-rabbit STAR 635P 1:300 (2-0012-007-2, Abberior), and goat anti-mouse STAR 580 1:300 (2-0002-005-1, Abberior). Finally, coverslips were mounted using the ProLong Gold Antifade Mountant reagent (Thermo Fisher Scientific).

For STED imaging we used a Leica TCS SP8 system and a HC PL APO C2S 100x/1.40 oil objective. For detailed information about the imaging settings please refer to the chapter 'Confocal and STED immunofluorescence microscopy' above. In addition and prior to immunofluorescence STED microscopy, neighboring histological sections were stained with hematoxylin/eosin and sirius-red/fast-green by protocols described below, to verify tissue integrity, avoid areas with excessive fibrosis, and to identify sections that exhibit planar longitudinal orientations of cardiac myocytes.

Live membrane staining and image analysis

Isolated AMs were plated on laminin-coated coverslips and incubated for 10 minutes in nominally Ca^{2+} free perfusion buffer (Supplemental Table 2) containing either 40 µM di-8-ANEPPS (D3167, Invitrogen) (3) or 5 µM Chol-PEG-KK114 (custom synthesis) (5). Described previously in detail, Chol-PEG-KK114 was used at a concentration of 5 µM for bulk membrane labeling for STED microscopy. Next, cells were washed three times in perfusion buffer and imaged at room temperature (18-20 °C). Perfusion buffer containing 2,3-butanedione-monoxime (B0753, Sigma Aldrich) was used to inhibit myocyte contraction. For confocal imaging of TAT membrane structures we used di-8-ANEPPS, a Zeiss LSM 710 or Zeiss LSM 880 microscopy system, a Plan-Apochromat 63x/1.40 oil objective, and a pixel

size of 100 x 100 nm as described previously (4). For STED imaging of Chol-PEG-KK114 stained AMs, we used a Leica TCS SP8 microscopy system and a HC PL APO C2S 100x/1.40 oil objective. The STED workflow was optimized for the KK114-fluorophore using the following final parameters: a pixel size of 16.23 x 16.23 nm, a pixel dwell time of 400 ns, a scanning speed of 600 Hz, 32x line averaging, excitation by a white light laser at 635 nm, STED depletion at 775 nm, and fluorescence detection between 650-700 nm.

For TAT-network analysis, cells were manually aligned and ROIs from individual cells selected, while excluding the surface sarcolemmal membrane and the nuclei. 2D skeleton images from confocal live cell images of TAT membrane networks were extracted as follows: after background subtraction and smoothing, ROIs were binarized using a predefined threshold and consecutively skeletonized. TAT network density was calculated in Fiji using the plugin 'Analyze Skeleton (2D/3D)'. In addition, TAT network component orientations were determined via the plugin 'Directionality'. By definition, AT components correspond to 0° and TT components to 90° orientation relative to the main cell axis. The AT:TT ratio was calculated using a bin size of ± 3°. For further details about the TAT-network analysis please refer our published protocols (3, 4).

To determine AT width (transverse diameter) in Chol-PEG-KK114 stained AMs by STED imaging, ROIs of 50 x 30 pixels were manually aligned and analyzed by fluorescence intensity profiling. AT signal profiles were fitted by a 2-peak Gaussian function in OriginPro 8.5G to determine the AT width (FWHM) as described previously (5). In addition, to determine the width (FWHM) of AT-continuous tubule-stacking membrane superstructures in JP2-OE AMs, we determined the distance between the two outermost intensity maxima of individual membrane structures. Supplemental Figures 7A and 7B provide an overview of a variety of exemplary superstructures.

High-pressure freezing and electron tomography

Isolated mouse AMs were prepared for high-pressure freezing and electron tomography (ET) using customized protocols described previously (3). ET images were acquired at the Electron Microscopy Core Facility of the EMBL Heidelberg.

Combined axial tubule and Ca^{2+} imaging

Freshly isolated mouse AMs were plated on laminin-coated coverslips, and the Ca^{2+} concentration in Tyrode solution (Supplemental Table 2) was gradually increased to a final concentration of 1.2 mM. For combined live membrane and Ca^{2+} imaging, cells were incubated in Chol-PEG-KK114 (1 µM) for 10 minutes and fluo-4 AM (10 µM; F14201 Invitrogen) for 25 minutes as described previously (5). Following washing in Tyrode solution, images were acquired in a live imaging chamber equipped with two platinum electrodes using a LSM 880 confocal microscope (Carl Zeiss, Jena, Germany) with a Plan-Apochromat 63/1.40 oil objective at room temperature. The fluorescent dyes Chol-PEG-KK114 and fluo-4 AM were recorded through separate channels by transversal line scanning: Chol-PEG-KK114 was excited at 633 nm and detected between 638 - 747 nm; fluo-4 was excited at 488 nm and detected between 493 - 622 nm. The pinhole was set to 1 airy unit for fluo-4 (49 µm) and 1.48 for Chol-PEG-KK114 (90 µm). Excluding the nucleus, we used 20 µm sized transverse line scanning (100 pixels) at 0.806 ms per line. Following manual AM quality control for regular cell structure, striation, and contractility by field stimulation, systolic Ca^{2+} transients and spontaneous Ca^{2+} spark activity were recorded by and directly following electrical field stimulation (3 ms long, 23 V amplitude) at 1 Hz frequency. The ImageJ plugin SparkMaster (6) was used for Ca^{2+} spark detection using a threshold 3.8-times above the background standard deviation. To correlate Ca^{2+} sparks with membrane structures, the Chol-PEG-KK114 signal peaks were used to localize the sarcolemmal outer surface-membrane

versus the AT membranes to match the transversal position of individual Ca^{2+} sparks within the following boundaries: peak surface-membrane signal ± 1.25 µm; and AT peak signal ± 1 µm. The AT spark frequency was further normalized to the number of AT-structures in ROIs that excluded the surface membrane to account for AT-proliferation in shRNA-JP2 knock-down cells. To estimate SR Ca^{2+} load in WT vs. JP2-OE AMs, we used a caffeine dump protocol (10 mM) after 1 Hz field stimulation. SR Ca^{2+} load measurements were performed in the absence of Chol-PEG-KK114. Field-stimulated Ca^{2+} transients and the caffeine-induced Ca^{2+} transient traces were fitted and analyzed in OriginPro 8.5G.

In vivo 6-lead mouse electrocardiography

After induction of anesthesia with isoflurane in oxygen, mice were fixed to a temperature control plate in supine position. For ECG signal acquisition four electrodes were subcutaneously placed on each limb. During ECG recording, anesthesia was maintained at 1.5% isoflurane through a rodent ventilator (Harvard Apparatus MiniVent 845), and 6-leads were recorded (IOX 2.10.0.40, emka technologies). Raw data were processed using ECGauto (version 3.3.5.10, Emka Technologies) with a 50 Hz notch filter. Representative lead I ECG traces are shown as exemplary figure panels.

Sarcomere shortening of atrial myocytes

Freshly isolated atrial myocytes from WT vs. JP2-OE mice 4 weeks post-TAC were pipetted onto a glass coverslip in a live imaging chamber with platinum electrodes in Tyrode solution after Ca^{2+} reintroduction (1.2 mM) at room temperature. Only cells with a brick-like shape, a regular striation pattern, and cell-wide contractile activity were selected to image sarcomere shortening. We used an Eclipse TE2000-U microscope (Nikon) in combination with an optical shortening capture system (IonOptix, Milton, MA) for sarcomere shortening measurements. Intracellular ROIs were selected as large as possible. For sarcomere

shortening, atrial myocytes were field stimulated at 1 Hz by 3 ms long voltage steps (23 V). Sarcomere shortening was analyzed using IonWizard 6.5 (Ion Optix, Milton, MA).

Mouse echocardiography

Transthoracic echocardiography of the mouse heart left atrium and the left ventricle was performed under mild anesthesia (isoflurane 1.5% in oxygen). We used a 30 MHz transducer to digitally record the left parasternal long- and short-axis views. Left atrial recording used a left parasternal long-axis view as described previously (3). Body temperature, respiration rate, and surface ECG traces were monitored throughout the echocardiography procedure. Investigators were blinded for the treatment and the genotype of individual mice.

Cardiac immunoblot protein analysis

Mice were anesthetized with isoflurane and euthanized by cervical dislocation. Following extraction, hearts were perfused with perfusion buffer (Supplemental Table 2) for 2 min at 37 °C using a modified Langendorff setup to clear myocardial tissue from blood cells. Next, hearts were dissected and atrial and ventricular tissue was snap-frozen and stored at -80 °C. Mouse and human atrial or ventricular tissues were homogenized in ice-cold homogenization buffer (HEPES 10 mM, sucrose 300 mM, NaCl 150 mM, EGTA 1 mM, $CaCl_2$ 2 mM, Triton X-100 0.5% v/v, protease and phosphatase inhibitor mix (Roche), pH 7.4, using a Miccra D-1 homogenizer. The homogenates were centrifuged at 8,000 g for 10 minutes at 4 °C to obtain the post-nuclear fraction. Protein concentrations were determined via Pierce BCA Protein Assay Kit (Thermo Fisher Scientific). For Western blotting 25 µg of protein per lane were resolved by SDS-PAGE using 4-20% Tris-Glycine gradient protein gels (XP04205BOX, Thermo Fisher Scientific). Gels were electrophoresed at constant 200 V. Proteins were transferred onto PVDF membranes (0.45 mm, Immobilon-FL, Merck Millipore) using an electrophoretic transfer cell (1703930, Bio-Rad) at constant 100 V for a duration of 2 h in

transfer buffer (Tris 32.5 mM, glycine 192 mM) at 4 °C. Membranes were blocked for 1 h in 5% w/v non-fat milk in Tris-buffered saline with 0.05% v/v Tween 20, and incubated with the primary antibodies listed in Supplemental Table 1 at 4 °C overnight. After washing, blots were incubated with fluorescent anti-mouse, anti-rabbit or anti-goat secondary antibodies at a dilution of 1:15,000 for a minimum period of 1 hour at room temperature (P/N 926-32212, P/N 926-68072, P/N 926-32213, P/N 926-68073, P/N 926-32214, P/N 926-68074, IRDye LI-COR). Membranes were developed with the Odyssey CLx imaging system (LI-COR). Band densitometry analysis was performed using Image Studio Lite Version 5.2 and normalized to GAPDH.

Prior to blocking, membranes containing atrial samples were cut after Ponceau staining to allow for immuno-detection of different proteins due to the limiting amount of atrial tissue from mouse hearts. In addition, primary antibodies were characterized on full blots in preparation of the final experiments represented in the manuscript. Please see Supplemental Figure 1 for full scans of the Western blots reported.

Co-immunoprecipitation

Mouse whole heart lysates were solubilized with co-IP buffer: Tris 50 mM, NaCl 150 mM, CHAPS 0.15% w/v (Carl Roth, Germany), EGTA 1 mM, protease inhibitor mix (Roche), pH 7.4; 500 µg total protein was incubated with 5 µg anti-junctophilin-2 antibody (sc-377086, Santa Cruz Biotechnology) or normal mouse IgG (sc-2025, Santa Cruz Biotechnology) antibody at 4 °C overnight. Dynabeads Protein G (Thermo Fisher Scientific) were added and incubated for 2 h at 4 °C. Beads were washed thrice for 10 min with ice-cold co-IP buffer, and resuspended in 2 × SDS buffer containing β-mercaptoethanol. Samples were heated to 70 °C for 5 min and resolved on 4-20% Tris-Glycine gradient protein gels (XP04205BOX, Thermo Fisher Scientific). After transfer on PVDF membranes and blocking (please see above), we

applied the primary antibodies against junctophilin-2 (sc-377086, Santa Cruz Biotechnology) and $Ca_V1.2$ (ab 58552, Abcam) for protein detection. Please refer to Supplemental Table 1 for detailed antibody information. To reduce unspecific signals, $Ca_V1.2$ antibody incubation was combined with IRDye-680 detection reagent according to the Quick Western Kit manual (LI-COR).

Histology of mouse hearts

For histomorphological staining, dissected mouse heart tissues were fixed in Roti-Histofix 4 % overnight (Carl Roth, Germany), embedded in paraffin, and cut into 4 µm thick histological sections. After deparaffinization and rehydration, samples were stained with hematoxylin-eosin. To visualize interstitial, perivascular, and endo-/epicardial fibrosis, histological sections were labeled with sirius-red/fast-green (collagen staining kit 9046, amsbio) as per the manufacturer's instructions.

References

1. van Oort RJ, Garbino A, Wang W, Dixit SS, Landstrom AP, Gaur N, De Almeida AC, Skapura DG, Rudy Y, Burns AR, et al. Disrupted junctional membrane complexes and hyperactive ryanodine receptors after acute junctophilin knockdown in mice. Circulation. 2011;123(9):979-88.
2. Hu P, Zhang D, Swenson L, Chakrabarti G, Abel ED, and Litwin SE. Minimally invasive aortic banding in mice: effects of altered cardiomyocyte insulin signaling during pressure overload. Am J Physiol Heart Circ Physiol. 2003;285(3):H1261-9.
3. Brandenburg S, Kohl T, Williams GS, Gusev K, Wagner E, Rog-Zielinska EA, Hebisch E, Dura M, Didie M, Gotthardt M, et al. Axial tubule junctions control rapid calcium signaling in atria. J Clin Invest. 2016;126(10):3999-4015.
4. Wagner E, Brandenburg S, Kohl T, and Lehnart SE. Analysis of tubular membrane networks in cardiac myocytes from atria and ventricles. J Vis Exp. 201492):e51823.
5. Brandenburg S, Pawlowitz J, Fakuade FE, Kownatzki-Danger D, Kohl T, Mitronova GY, Scardigli M, Neef J, Schmidt C, Wiedmann F, et al. Axial Tubule Junctions Activate Atrial Ca(2+) Release Across Species. Front Physiol. 2018;9(1227.
6. Picht E, Zima AV, Blatter LA, and Bers DM. SparkMaster: automated calcium spark analysis with ImageJ. Am J Physiol Cell Physiol. 2007;293(3):C1073-81.

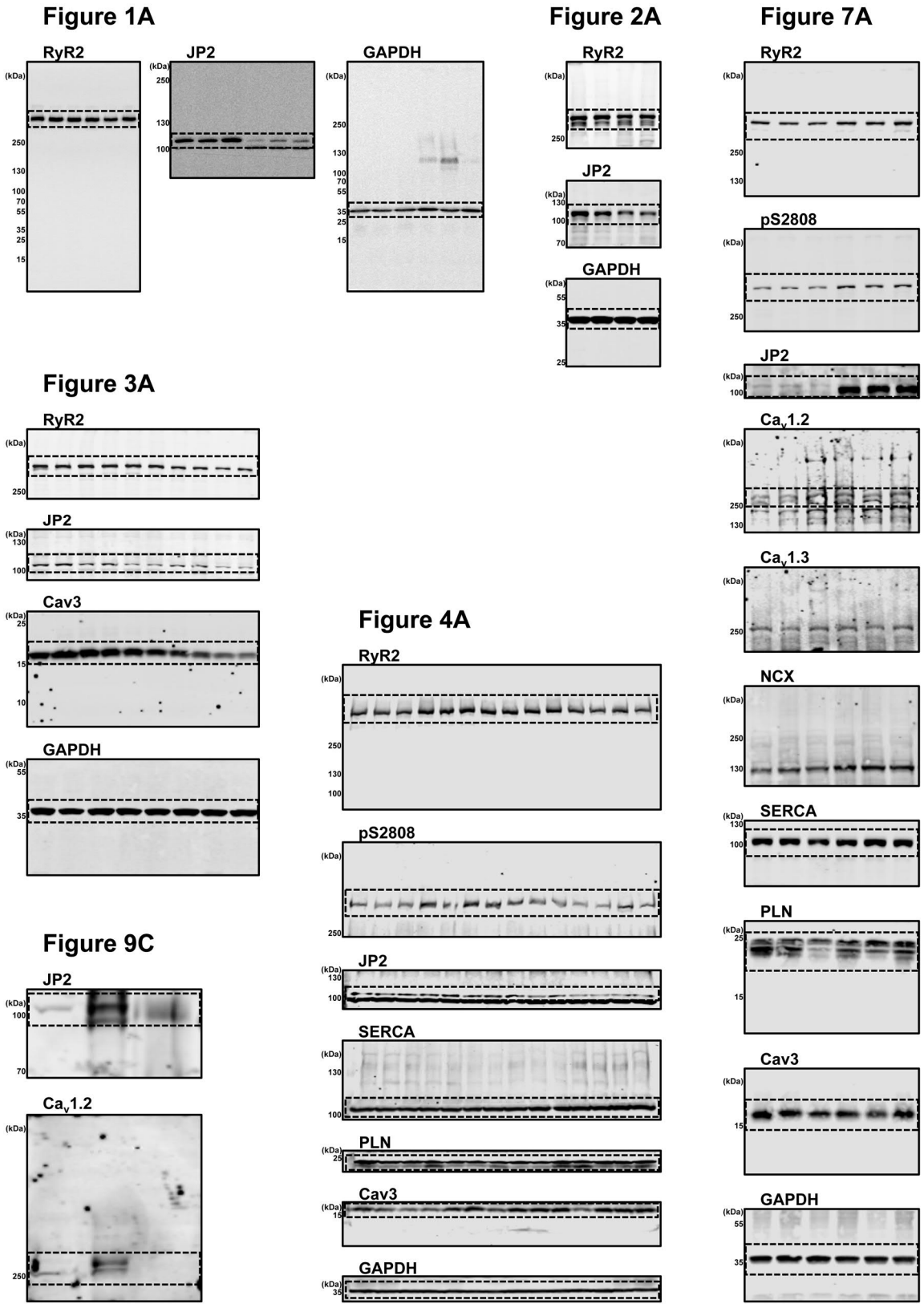

Supplemental Figure 1. Documentation of full scans of Western blots. Dashed frames indicate the data presented as manuscript Figures.

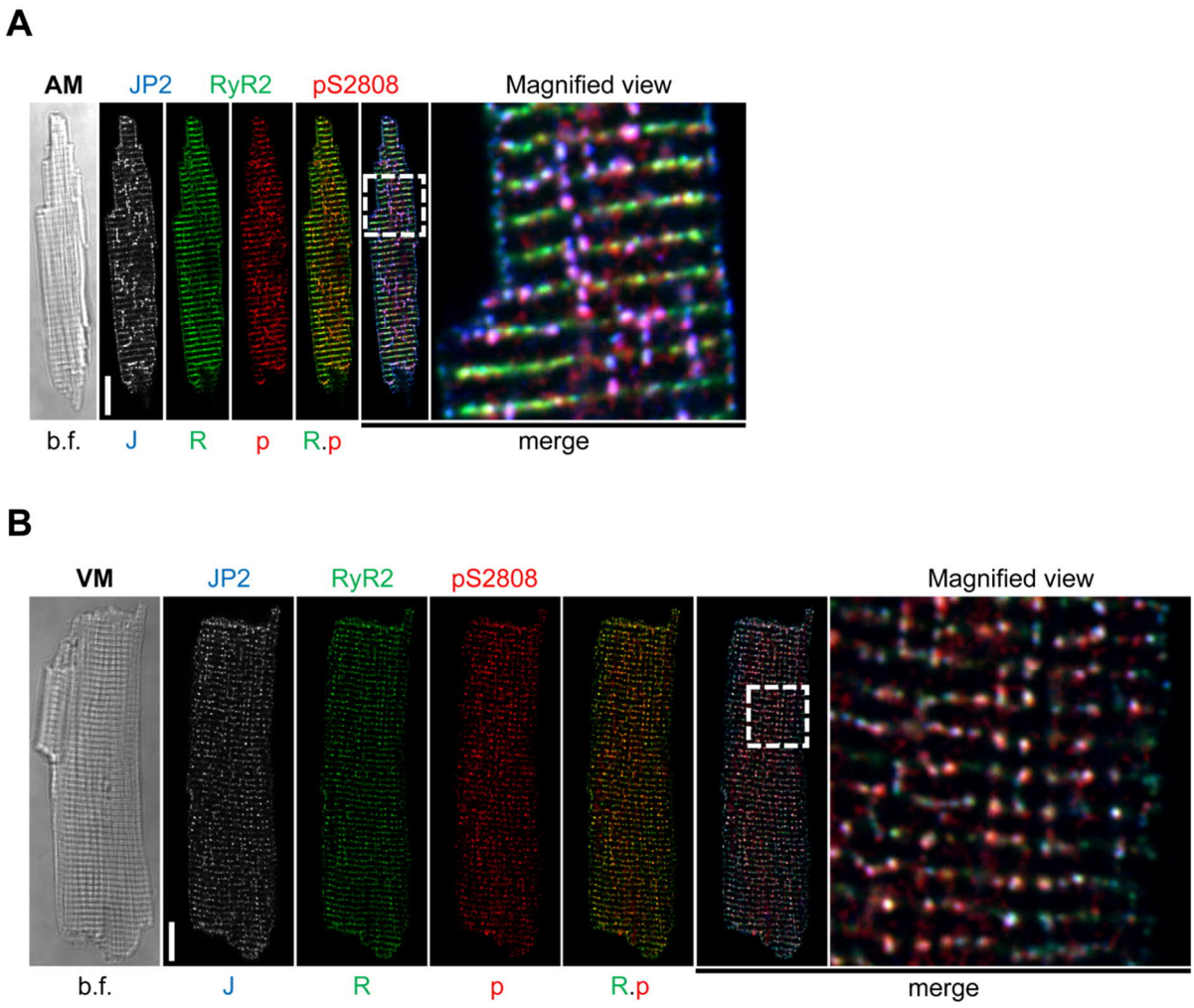

Supplemental Figure 2. Larger junctophilin-2 clusters co-localize with highly phosphorylated RyR2 clusters in atrial myocytes. (**A**) Confocal imaging of an isolated atrial myocyte (AM) triple-stained for junctophilin-2 (JP2), ryanodine receptor (RyR2) and the protein kinase A phosphorylated RyR2-Ser2808 (pS2808) epitope. Larger junctophilin-2 clusters co-localize with highly phosphorylated RyR2-pS2808 clusters (violet) on axially aligned string-of-pearl arrangements deep inside AMs. The majority of RyR2 clusters occurring in transverse striations, however, are rarely phosphorylated at Ser2808 or co-localized with junctophilin-2 clusters. (**B**) The majority of ventricular myocyte (VM) RyR2 clusters appears to co-localize with abundant junctophilin-2 clusters. Dashed boxes indicate magnified views on the right. Bright field (b.f.) images document the structural cell quality after isolation and PFA fixation. Scales 10 µm.

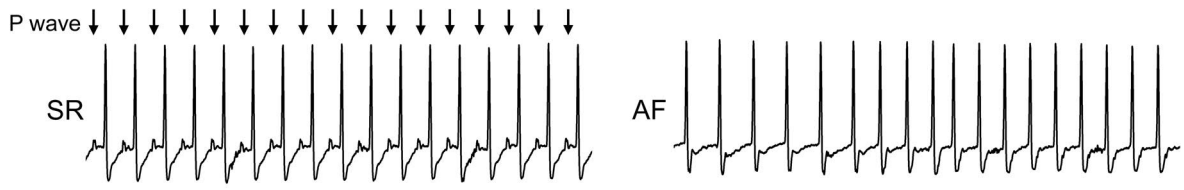

Supplemental Figure 3. Episodes of spontaneous intermittent atrial rhythm disorders post-TAC. 6-lead-ECG recording traces show normal sinus rhythm (SR, *left*) versus spontaneous episode of paroxysmal atrial fibrillation (AF, *right*) post-TAC. Within 10 min ECG recording, 3 out of 27 TAC mice presented spontaneous episodes of paroxysmal arrhythmias, converting spontaneously into normal sinus rhythm. Shown are 2 s ECG lead I traces. Arrows indicate regular P-waves.

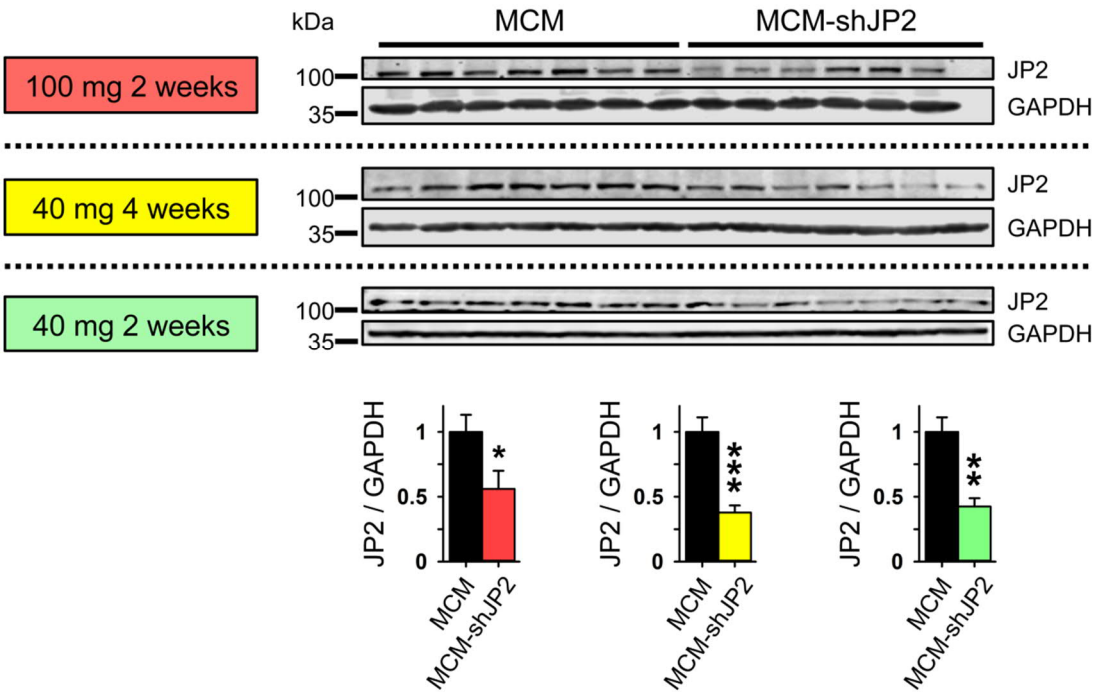

Supplemental Figure 4. Comparison of three different protocols for atrial shRNA-mediated junctophilin-2 knock-down *in vivo*. We tested different doses of tamoxifen (single injection of 40 versus 100 mg/kg body weight i.p.) and different durations of tamoxifen treatment (2 versus 4 weeks). The primary objective was to decrease atrial junctophilin-2 protein expression by at least 50% using a cardiomyocyte-restricted junctophilin-2 knock-down system reported previously (1). Immunoblots of atrial tissue lysates obtained from MCM control versus MCM-shJP2 knock-down hearts revealed similar junctophilin-2 protein levels 2 and 4 weeks after 40 mg tamoxifen treatment. Finally, to avoid lethal heart failure from ventricular junctophilin-2 knock-down, MCM and MCM-shJP2 mouse data presented throughout Figures 4-6 were treated for 2 weeks by one-time i.p. injection of 40 mg tamoxifen per kg body weight. NS, not significant; *p<0.05; **p<0.01; ***p<0.001; Student's *t* test.

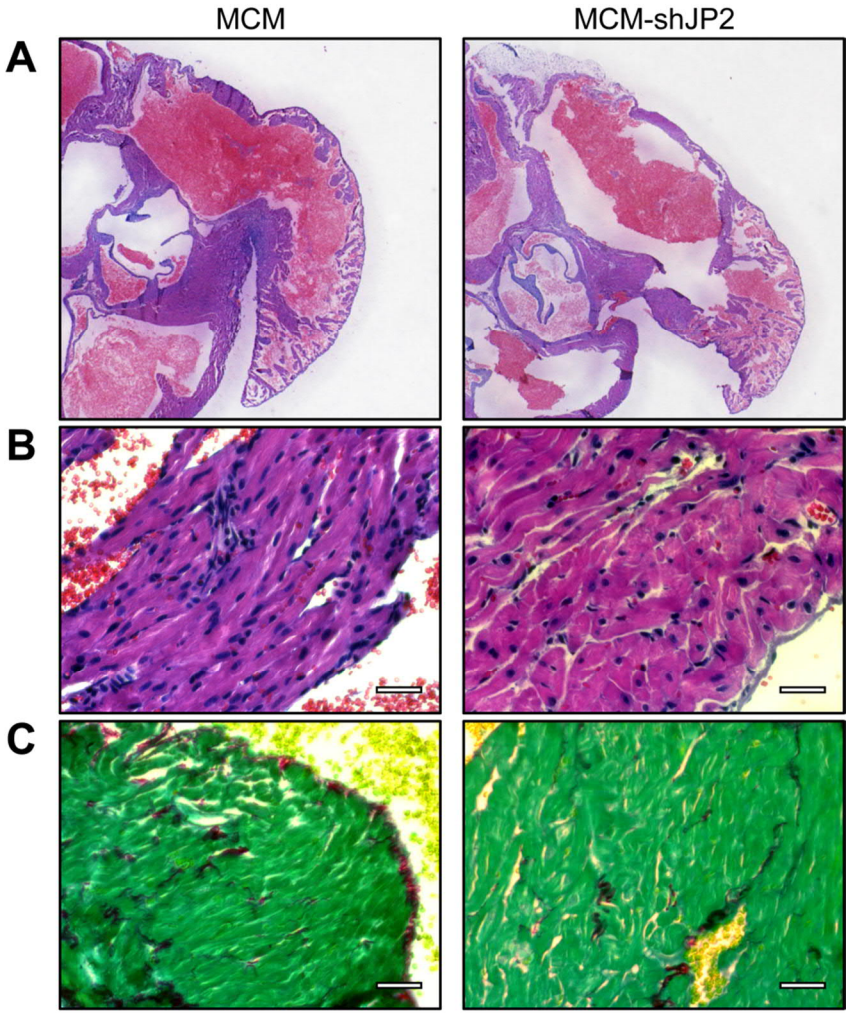

Supplemental Figure 5. Histologic analysis in junctophilin-2 knock-down versus control atria. (**A**) Control (MCM) and junctophilin-2 knock-down (MCM-shJP2) hearts were sectioned at the level of the aortic root and stained with Hematoxylin-Eosin (HE). The images represent left atrial sections. Notably, junctophilin-2 knock-down did not result in significant atrial dilation or hypertrophy compared to MCM control. (**B**) Magnified views of HE stained left atrial sections show normal myocyte dimensions. (**C**) Sirius-Red/Fast-Green staining did not reveal increased fibrosis in junctophilin-2 knock-down left atria. All scales 20 µm.

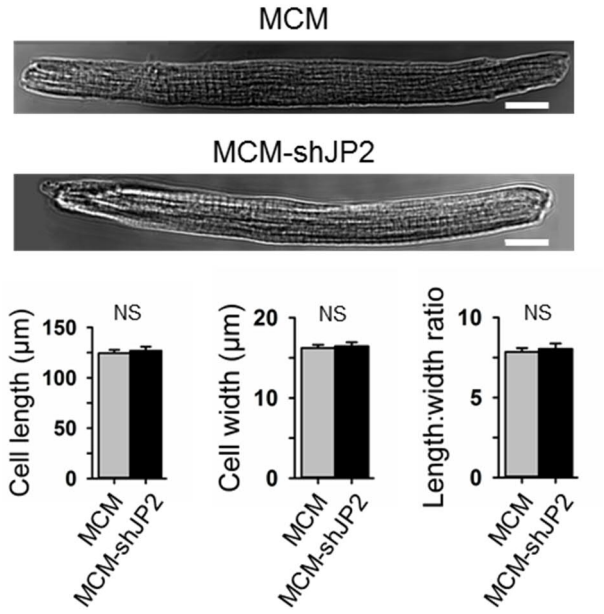

Supplemental Figure 6. Dimensions of atrial myocytes after junctophilin-2 knock-down. *Top:* Representative bright field images of isolated atrial myocytes from control (MCM) versus junctophilin-2 knockdown (MCM-shJP2) hearts. Scales 10 µm. *Bottom:* Bar graphs comparing cell length, width and length-to-width ratio. n = 54 MCM and 56 MCM-shJP2 AMs from three hearts each. NS, not significant; Student's *t* test.

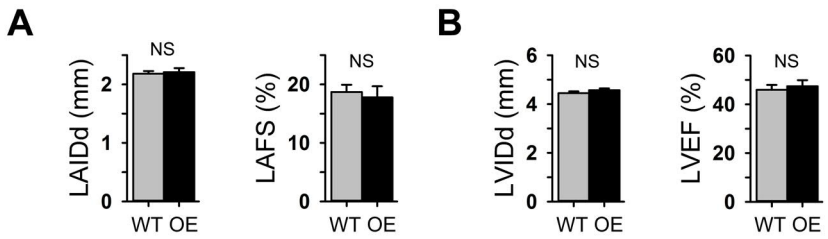

Supplemental Figure 7. Echocardiographic analysis of transgenic junctophilin-2 overexpressor mice. (**A**) Left atrial (LA) and (**B**) left ventricular (LV) echocardiography showed normal heart dimensions and functions in JP2-OE mice. IDd, inner diameter in diastole; FS, fractional shortening; EF, ejection fraction. n=11 WT and 9 JP2-OE mice. NS, not significant, Student's t test.

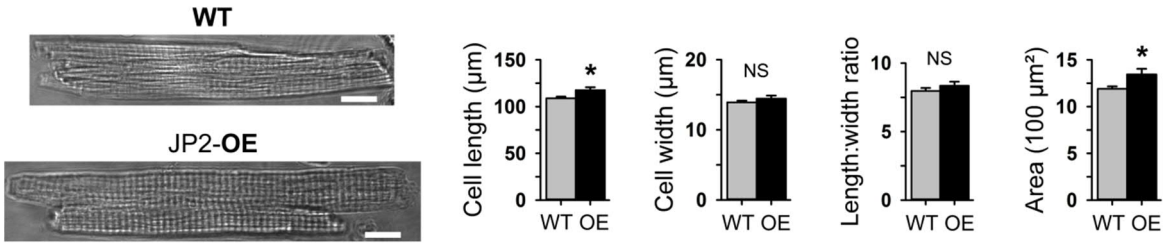

Supplemental Figure 8. Junctophilin-2 overexpression mildly increases the length of atrial myocytes. *Left:* Bright field images of isolated atrial myocytes obtained from wild-type (WT) versus junctophilin-2 overexpression (JP2-OE) hearts. Scales 10 µm. *Right:* Bar graphs analyzing cell length, width, length-to-width ratio and area. n = 55 WT and 41 JP2-OE AMs from three hearts each. NS, not significant; *$p<0.05$, Student's t test.

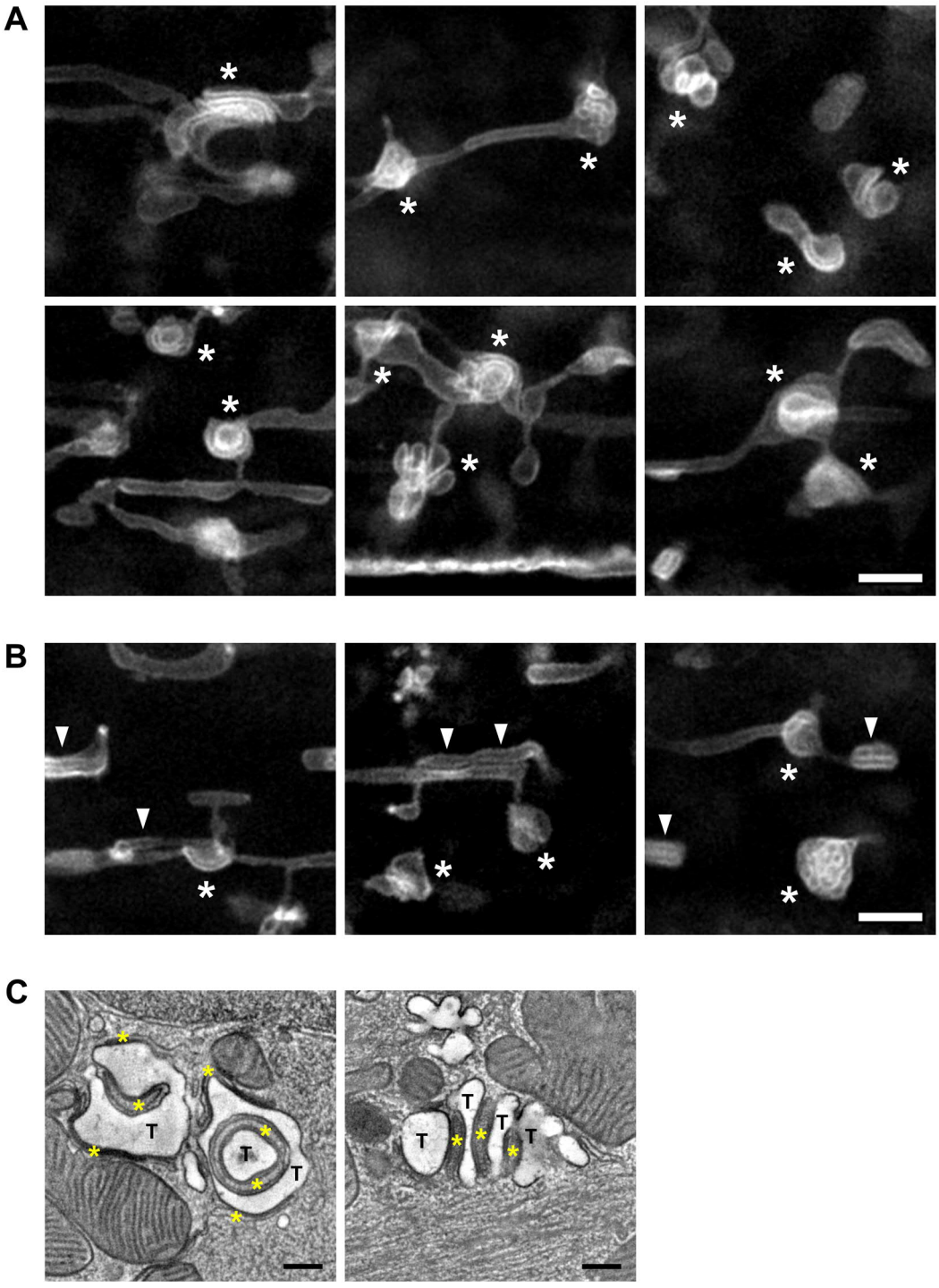

Supplemental Figure 9. Junctophilin-2 overexpression induces extensive tubular membrane folding on axial tubule structures in atrial myocytes. (**A**) Live STED nanoscopy of isolated AMs obtained from junctophilin-2 overexpression hearts and stained with the membrane dye Cholesterol-PEG-KK114. Within the intracellular TAT network, asterisks identify complex folded tubular membrane superstructures continuous with axial tubules in (**A-B**). (**B**) In addition, arrowheads point to segments in which two axial tubules run directly next to each other. Stacks of tubular membrane structures and paired axial tubules were characteristically found in JP2-OE AMs. (**C**) ET images display individual membrane superstructures that contain coiled or stacked tubule (T) components in JP2-OE cells, closely intercalating SR membrane structures (yellow asterisks) containing RyR2 channel densities. *Left:* Circular tubule cross section surrounded by SR membranes. *Right:* Stack of tubule structures tightly intercalated by SR membranes. Scales 1 µm (**A-B**) and 200 nm (**C**).

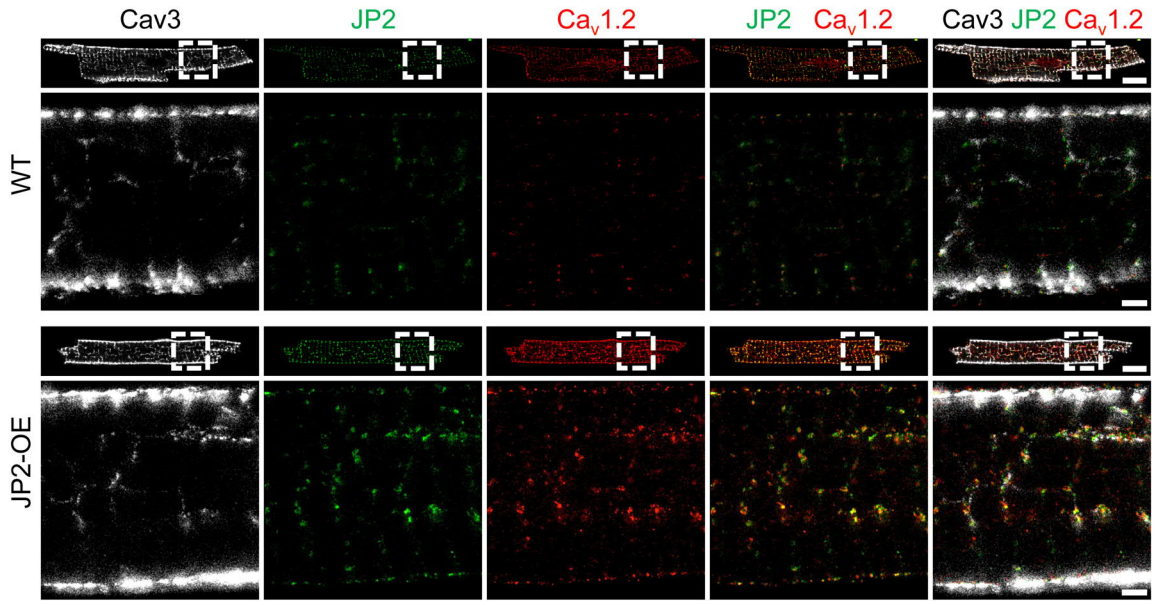

Supplemental Figure 10. Increased $Ca_V1.2$ channel clustering on axial tubules in atrial myocytes overexpressing junctophilin-2. STED imaging of isolated atrial myocytes triple-stained for caveolin-3 (Cav3), junctophilin-2 (JP2) and the L-type Ca^{2+} channel isoform $Ca_V1.2$. In JP2-OE cells, larger $Ca_V1.2$ clusters were highly co-localized with junctophilin-2 on axial tubules as compared to WT cells. Images are representative of three independent cell isolations. Dashed boxes indicate magnified views below. Scales: 10 µm in cell overviews and 1 µm in magnifications.

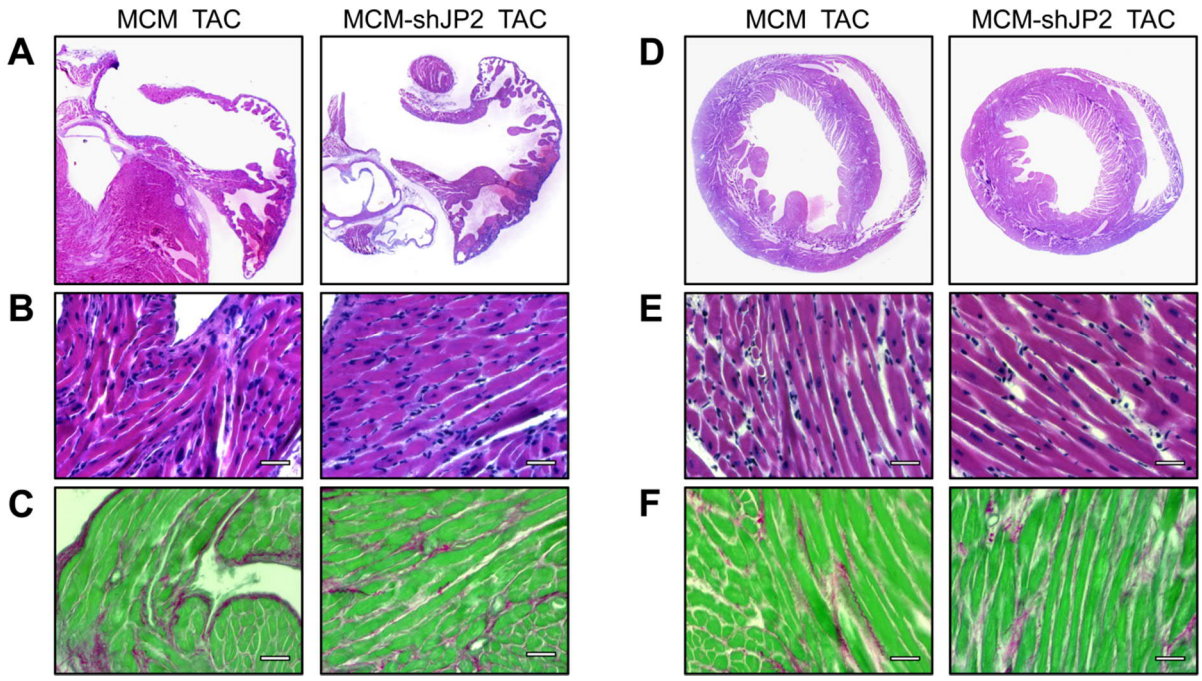

Supplemental Figure 11. Histology of junctophilin-2 knock-down hearts 2 weeks post TAC. (**A**) Representative histological sections showing the left atrium (**A-C**) and left ventricle (**D-F**) in control (MCM) versus junctophilin-2 knock-down (MCM-shJP2) hearts from mice, which died 2 weeks post TAC surgery. (**A**) Hearts were sectioned at the level of the aortic root and stained with Hematoxylin-Eosin (HE). Junctophilin-2 knock-down hearts did not show any significant dilation or hypertrophy compared to MCM control. Moreover, (**B**) magnified views reveal similar cell dimensions in HE stained tissue, and (**C**) moderate fibrosis in Sirius-Red/Fast-Green collagen stained tissue of both MCM versus MCM-shJP2 atria. (**D**) Transverse mid-ventricular sections from the same hearts as shown in (**A-C**) stained with HE. (**E**) Magnified views of ventricular HE stained sections, and (**F**) Sirius-Red/Fast-Green collagen stained sections. Scales 20 µm.

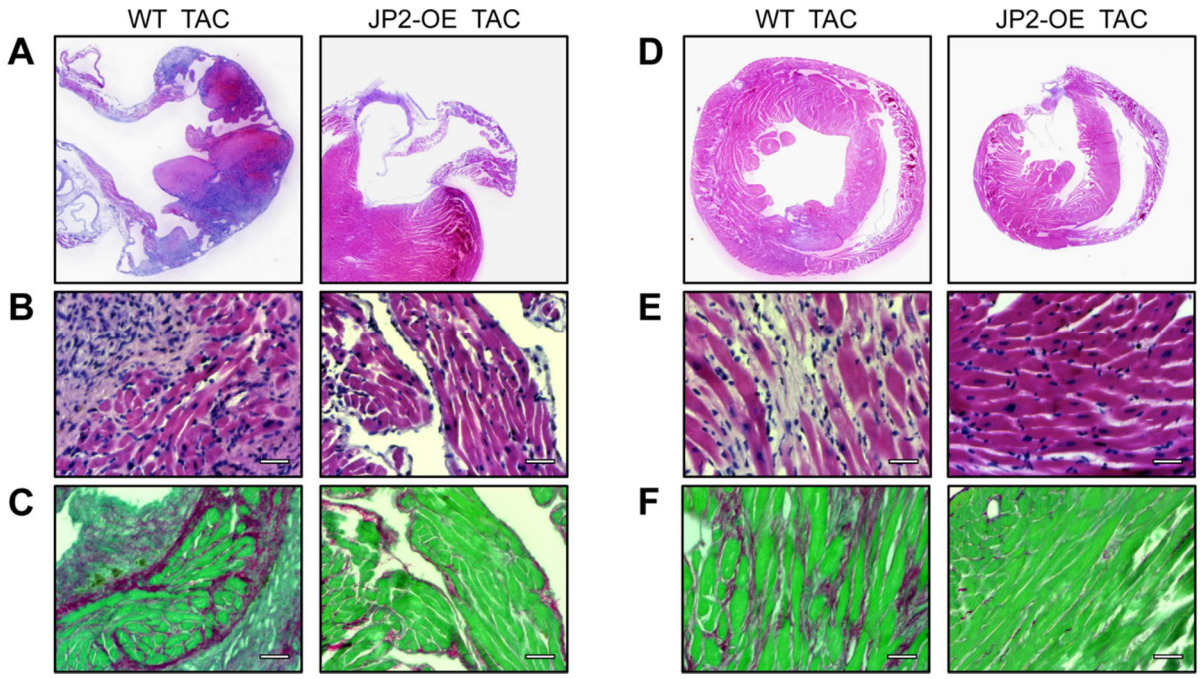

Supplemental Figure 12. Junctophilin-2 overexpression attenuates histomorphological remodeling in the atria and ventricles 4 weeks post-TAC. (**A**) Representative histological sections showing the left atrium (**A-C**) and left ventricle (**D-F**) in wild-type (WT) versus junctophilin-2 overexpression (JP2-OE) hearts from mice 4 weeks post-TAC. (**A**) Hearts were sectioned at the level of the aortic root and stained with Hematoxylin-Eosin (HE). JP2-OE atria were significantly smaller compared to WT atria. In addition, (**B**) magnified views of HE stained sections show a well-organized thrombus inside the WT left atrial appendage. (**C**) Sirius-Red/Fast-Green collagen stained sections revealed substantial interstitial fibrosis in the WT heart, which was significantly reduced in JP2-OE hearts. (**D**) Transverse mid-ventricular sections from the same hearts as shown in (**A-C**) stained with HE. (**E**) Magnified views of ventricular HE and (**F**) Sirius-Red/Fast-Green collagen stained sections. Scales 20 µm.

Protein of interest	Species	Clonality	Clone	Antigen / Immunogen	Company	Catalog no.	Concentration	Dilution WB	Dilution IF	IF cross reaction
$Ca_v1.2$	rabbit	polyclonal		peptide (C)TTKINMDDLQPSENEDKS, corresponding to amino acid residues 848-865 of rat $Ca_v1.2$	Alomone labs	ACC-003	0.8 mg/ml	1:200	1:500	yes (nucleus)
$Ca_v1.2$	rabbit	polyclonal		synthetic peptide corresponding to rat CACNA1C aa. 818-835 conjugated to Keyhole Limpet Haemocyanin (KLH).	Abcam	ab58552	0.8 mg/ml	1:500		
$Ca_v1.3$	rabbit	polyclonal		peptide (C)DNKVTIDDYQEEAEDKD, corresponding to aa. residues 859-875 of rat $Ca_v1.3$, intracellular loop between domains II and III	Alomone labs	ACC-005	0.85 mg/ml	1:250		
Caveolin-3	mouse	monoclonal	26/ Caveolin 3	rat Caveolin 3 aa. 3-24	BD Biosciences	610421	250 µg/ml		1:500	no
Caveolin-3	rabbit	polyclonal		synthetic peptide aa. 1-18 of rat Caveolin 3	Abcam	ab2912	1 mg/ml	1:1000	1:500	no
Gapdh	mouse	monoclonal	6C5		Biotrend	5G4 Mab6C5	5.3 mg/ml	1:160,000		
Junctophilin-2	rabbit	polyclonal		synthetic peptide derived from C-terminal region of mouse Junctophilin 2	Thermo Fisher Scientific	40-5300	0.25 mg/mL	1:1000	1:500	no
Junctophilin-2	goat	polyclonal		against C-terminus of Junctophilin2	Santa Cruz Biotechnology	sc-51313	200 µg/ml	1:200	1:200	no
Junctophilin-2	mouse	monoclonal	H-3	raised against aa. 431-680 mapping near the C-terminus of Junctophilin2 of human origin	Santa Cruz Biotechnology	sc-377086	200 µg/ml	1:500		
NCX1	Rabbit	polyclonal		antiserum was produced against canine cardiac sarcolemmal Na^+/Ca^{2+}-exchanger (NCX1; full length isolated protein)	Swant	π 11-13		1:1000		
Phospholamban	mouse	monoclonal	2D12	synthetic peptide corresponding to dog Phospholamban aa. 2-25	Abcam	ab2865		1:2500		
Ryanodine Receptor 2	mouse	monoclonal	C3-33	canine cardiac RyR	Thermo Fisher Scientific	MA3-916	1 mg/ml		1:500	no
Ryanodine Receptor 2	rabbit	polyclonal		aa. QDEVRGDGEEGERKPLEAALPSEDLTDLKELTE ESDLLSDIFGLDLKREGGQYKLIPHNPNAGLSDLMS NPVPMPEVQEKFQEQKAKEEEKEEKEETKSEPE	Sigma-Aldrich	HPA020028	0.18 mg/ml	1:2500	1:500	no
Ryanodine Receptor 2 phosphoSerin2808	rabbit	polyclonal		synthetic peptide (YNRTRRIS(PO3H2)QT2810) conjugated to keyhole limpet haemocyanin	Badrilla Ltd.	A010-30		1:1000	1:250	yes (nucleus)
Serca2a	rabbit	polyclonal		synthetic peptide (C-LEPAILE997) corresponding to amino acid at the extreme C-terminus of SERCA2a	Badrilla Ltd.	A010-20		1:1000		

Supplemental Table 1. Documentation of primary antibodies used for Western blotting (WB) and immunofluorescence imaging (IF).

Perfusion buffer	NaCl 120.4 mM, KCl 14.7 mM, KH_2PO_4 0.6 mM, Na_2HPO_4 0.6 mM, $MgSO_4$ 1.2 mM, HEPES 10 mM, $NaHCO_3$ 4.6 mM, taurine 30 mM, 2,3-butanedione-monoxime 10 mM, glucose 5.5 mM, pH 7.4 (adjusted with NaOH)
Tyrode solution	NaCl 140 mM, KCl 5.4 mM, $MgCl_2$ 1.2 mM, HEPES 10 mM, Na_2HPO_4 0.33 mM, $CaCl_2$ 1.2 mM, glucose 10 mM, pH 7.4, (adjusted with NaOH)

Supplemental Table 2. Composition of physiological buffer solutions as referenced in the methods section.

	Figure 2B	**Figure 2C *top***	**Figure 2C *bottom***
Indication for heart surgery	AVD	CAD	CAD
Heart tissue	left atrium	right atrium	left ventricle
Gender, m/f	m	m	m
Age, y	81	50	71
Body mass index, kg/m^2	25	35	24
Hypertension	+	+	+
Diabetes	+	-	-
Hyperlipidemia	+	+	+
LVEF, %	60	60	52
Atrial fibrillation	permanent	-	-
Digitalis	+	-	-
ACE inhibitors	+	+	+
AT1 blockers	-	-	-
β-Blockers	+	+	+
Dihydropyridines	-	-	+
Diuretics	+	+	-
Nitrates	-	-	-
Lipid-lowering drugs	+	+	+

Supplemental Table 3. Clinical patient information. Human cardiac tissue samples were obtained from patients undergoing open heart surgery for aortic valve replacement or bypass grafting, respectively. AVD, aortic valve disease; CAD, coronary artery disease; LVEF, left ventricular ejection fraction; ACE, angiotensin-converting enzyme; AT, angiotensin receptor.